

Feature Extraction Approaches for Biological Sequences: A Comparative Study of Mathematical Models

Robson Parmezan Bonidia^{a,b,*}, Lucas Dias Hiera Sampaio^a, Douglas Silva Domingues^a, Alexandre Rossi Paschoal^a, Fabrício Martins Lopes^a, André Carlos Ponce de Leon Ferreira de Carvalho^b, Danilo Sipoli Sanches^a

^a*Department of Computer Science, Bioinformatics Graduate Program (PPGBIOINFO), Federal University of Technology - Paraná, UTFPR, Campus Cornélio Procópio, Brazil.*

^b*Institute of Mathematics and Computer Sciences, University of São Paulo - USP, São Carlos, 13566-590, Brazil*

Abstract

The number of available biological sequences has increased significantly in recent years due to various genomic sequencing projects, creating a huge volume of data. Consequently, new computational methods are needed to analyze and extract information from these sequences. Machine learning methods have shown broad applicability in computational biology and bioinformatics. The utilization of machine learning methods has helped to extract relevant information from various biological datasets. However, there are still several obstacles that motivate new algorithms and pipeline proposals, mainly involving feature extraction problems, in which extracting significant discriminatory information from a biological set is challenging. Considering this, our work proposes to study and analyze a feature extraction pipeline based on mathematical models (Numerical Mapping, Fourier, Entropy, and Complex Networks). As a case study, we analyze Long Non-Coding RNA sequences. Moreover, we divided this work into two studies, e.g., (I) we assessed our proposal with the most addressed problem in our review, e.g., lncRNA vs. mRNA; (II) we tested its generalization on different classification problems, e.g., circRNA vs. lncRNA. The experimental results demonstrated three main contributions: (1) An in-depth study of several mathematical models;

*Corresponding author

Email addresses: rbonidia@gmail.com (Robson Parmezan Bonidia), danilosanches@utfpr.edu.br (Danilo Sipoli Sanches)

(2) a new feature extraction pipeline and (3) its generalization and robustness for distinct biological sequence classification.

Keywords: Feature Extraction; Long Non-Coding RNAs; Biological Sequences; Numerical Mapping Techniques; Fourier; Complex Networks; Shannon; Tsallis.

¹ 1. Background

² In recent years, due to advances in DNA sequencing, an increasing number
³ of biological sequences have been generated by thousands of sequencing
⁴ projects [1], creating a huge volume of data [2]. During the last decade,
⁵ Machine Learning (ML) methods have shown broad applicability in computational
⁶ biology and bioinformatics [3]. Consequently, the ability to process
⁷ and analyze biological data has advanced significantly [4]. Tools have been
⁸ applied in gene networks, protein structure prediction, genomics, proteomics,
⁹ protein-coding genes detection, disease diagnosis, and drug planning [5, 6].
¹⁰ Fundamentally, ML investigates how computers can learn (or improve their
¹¹ performance) based on the data. Moreover, ML is a specialization of computer
¹² science related to pattern recognition and artificial intelligence [7].

¹³ Based on this, several works have focused on investigating sequences of
¹⁴ DNA and RNA molecules [8, 9, 10]. Applying ML methods in these sequences
¹⁵ has helped to extract important information from various datasets to explain
¹⁶ biological phenomena [3]. The development of efficient approaches benefits
¹⁷ the mathematical understanding of the structure of biological sequences [1],
¹⁸ e.g., Precision cancer diagnostics [11], analytics in plants [12], and Coronaviruses epidemic [13, 14]. However, according to [3, 15], there are still several
¹⁹ challenging biological problems that motivated the emergence of proposals
²⁰ for new algorithms. Fundamentally, biological sequence analysis with ML
²¹ presents one major problem, e.g., Feature Extraction [16], an inevitable process,
²² especially in the stage of biological sequence preprocessing [10, 17].

²⁴ Feature extraction seeks to generate a feature vector, optimally transforming
²⁵ the input data [16]. This procedure is exceptionally relevant for the success
²⁶ of the ML application because another primary goal is to extract important
²⁷ information from input data compactly, as well as removing noise and redundancy
²⁸ to increase the accuracy of ML models [18, 16]. Necessarily, several methods in
²⁹ bioinformatics apply ML algorithms for sequence classification, and as many
³⁰ algorithms can deal only with numerical data, sequences

31 need to be translated into sequences of numbers.

32 Thereby, modern applications extract relevant features from sequences
33 based on several biological properties, e.g., physicochemical, Open Reading
34 Frames (ORF)-based, usage frequency of adjoining nucleotide triplets, GC
35 content, among others. This approach is common in biological problems, but
36 these implementations are often difficult to reuse or adapt to another specific
37 problem, e.g., ORF features are an essential guideline for distinguishing Long
38 non-coding RNAs (lncRNA) from protein-coding genes [19], but not useful
39 features for classifying lncRNA classes [20, 21] (e.g., in [21], ORF score (fea-
40 ture importance) is less than 0.009 to classify circular RNA from other types
41 of lncRNAs). Consequently, the feature extraction problem arises, in which
42 extracting a set of useful features that contain significant discriminatory in-
43 formation becomes a fundamental step in the construction of a predictive
44 model [22].

45 Therefore, these problems make the process of biological sequence clas-
46 sification a challenging task, creating a growing need to develop new tech-
47 niques and methods to analyze sequences effectively and efficiently. Thereby,
48 this work studies the performance of different feature extraction methods
49 for biological sequence analysis, using mathematical models, e.g., numerical
50 mapping, Fourier transform, entropy, and graphs. As a case study, we will
51 use lncRNA sequences, which are fundamentally unable to produce proteins
52 [23] and have recently casted doubt on its functionality [24].

53 LncRNAs present several problem classes (e.g., lncRNA vs. mRNA [25,
54 26] and lncRNA vs. circRNA [27]), thus enabling us to create a scenario to
55 answer the questions raised in this work. Fundamentally, our main objective
56 is to propose generalist techniques, demonstrating their efficiency concerning
57 biological features. We consider biological approaches, those characteristics
58 that present a bias to the analyzed problem or some biological explanation,
59 e.g., ORF for lncRNA vs. mRNA [6, 19], as well as mathematical approaches
60 and information quantity measures such as entropy. Based on this context
61 and objectives, we assume the following hypothesis:

62 • **Hypothesis:** Feature extraction approaches based on mathematical
63 models are as efficient and generalist as biological approaches.

64 Considering this, our work contributes to the area of computer science
65 and bioinformatics. Specifically, it introduces new ideas and analysis for
66 the feature extraction problem in biological sequences. Thereby, we present

67 four new contributions: (1) A feature extraction pipeline using mathematical
68 models; (2) Analysis of 9 mathematical models; (3) Analysis of 6 numerical
69 mappings with Fourier, proposing statistical characteristics; (4) The general-
70 ization and robustness of mathematical approaches for the feature extraction
71 in biological sequences.

72 2. Related Works

73 Essentially, as emphasized, we adopt lncRNA sequences as a case study,
74 a class of Non-Coding RNAs (ncRNAs). Fundamentally, ncRNAs are un-
75 able to produce proteins. However, these ncRNAs contain unique informa-
76 tion that produces other functional RNA molecules [28, 23]. Moreover, they
77 demonstrate essential roles in cellular mechanisms, playing regulatory roles
78 in a wide variety of biological reactions and processes [29, 28]. The ncR-
79 NAs can be classified by length into two classes: Long Non-Coding RNA
80 (lncRNA - 200 nucleotides (nt) or more) and short ncRNA (less than 200
81 nt) [30, 31]. The lncRNAs are sequences with a length greater than 200 nu-
82 cleotides [32], and according to recent studies, play essential roles in several
83 critical biological processes [33, 34, 35], including transcriptional regulation
84 [36], epigenetics [37], cellular differentiation [38], and immune response [39].
85 Moreover, they are correlated with some complex human diseases, such as
86 cancer and neurodegenerative diseases [6, 40, 41].

87 In plants, according to [6, 42], the lncRNAs act in gene silencing, flowering
88 time control, organogenesis in roots, photomorphogenesis in seedlings, stress
89 responses [43, 44], and reproduction [45]. Furthermore, lncRNAs are present
90 in large numbers in genome [46] and have similar sequence characteristics
91 with protein-coding genes, such as 5' cap, alternative splicing, two or more
92 exons [47], and polyA+ tails [48]. They are also observed in almost all living
93 beings, not only in animals and plants but also yeasts, prokaryotes, and even
94 viruses [49, 50].

95 According to [46], lncRNAs do not contain functional ORFs. However,
96 recent studies have found bifunctional RNAs [51], raising the possibility that
97 many protein-coding genes may also have non-coding functions. Further-
98 more, lncRNAs can be grouped into five broad categories. The classifi-
99 cation occurs conforming to the genomic location, that is, where they are
100 transcribed, concerning well-established markers, e.g., protein-coding genes.
101 Among the categories are [52, 47]: sense, antisense, bidirectional, intronic,
102 intergenic. The genomic context does not necessarily provide some informa-

103 tion about the lncRNAs function or evolutionary origin; nevertheless, it can
104 be used to organize these broad categories [53].

105 In this context, we have conducted an in-depth review of the lncRNAs
106 classification methods, in which several approaches have been developed,
107 such as: CPC [54], CPAT [55], CNCI [56], PLEK [57], LncRNA-MFDL
108 [58], LncRNA-ID [59], LncRScan-SVM [60], LncRNAPred [61], DeepLNC
109 [62], PlantRNA_Sniffer [63], PLncPRO [64], RNAPlonc [65], BASiNET [66],
110 LncFinder [26], CREMA [67], LncRNAnet [19], CNIT [68], PLIT [69], PredLnc-
111 GFStack [70], LGC [71] and DeepCPP [72]. For better understanding, Figure
112 1 presents theses works divided into Mathematical, Biological, and Hybrid
113 approaches.

114 The CPC uses the extent and quality of the ORF, and derivation of the
115 BLASTX [73] search to measure the protein-coding potential of a transcript.
116 In the classification, the authors applied the LIBSVM package to train a Sup-
117 port Vector Machine (SVM) model, using the standard radial basis function
118 kernel. CPAT classifies transcripts of coding and non-coding using the Logis-
119 tic Regression (LR) classifier. This approach implements four features: ORF
120 coverage, ORF size, hexamer usage bias, and Fickett TESTCODE statis-
121 tic. CNCI was induced with SVM and applies profiling Adjoining Nucleotide
122 Triplets, and most-like CDS (MLCDS).

123 In contrast, PLEK (2014) is based on the k-mer scheme ($k = 1, \dots, 5$)
124 to predict lncRNA, also applying the SVM classifier. LncRNA-MFDL uses
125 Deep Learning (DL) and multiple features, among them: ORF, K-mer ($k =$
126 1, 2, 3), secondary structure (minimum free energy), and MLCDS. LncRNA-
127 ID predicts lncRNAs with Random Forest (RF) through ORF (length and
128 coverage), sequence structure (Kozak motif), ribosome interaction, alignment
129 (profile Hidden Markov Model - profile HMM), and protein conservation.

130 LncRScan-SVM uses stop codon count, GC content, ORF (score, CDS
131 length and CDS percentage), transcript length, exon count, exon length, and
132 average PhastCons scores. LncRNAPred classified lncRNAs with RF and
133 features based on ORF, signal to noise ratio, k-mer ($k = 1, 2, 3$), sequence
134 length, and GC content. DeepLNC uses only the k-mer scheme with entropy
135 and Deep Neural Network (DNN). PlantRNA_Sniffer was developed in 2017
136 to predict Long Intergenic Non-Coding RNAs (lncRNAs). The method ap-
137 plied SVM and extracted features from ORF (proportion and length) and
138 nucleotide patterns.

139 PLncPRO is based on machine learning and uses RF. The features se-
140 lected include ORF quality (score and coverage), number of hits, significance

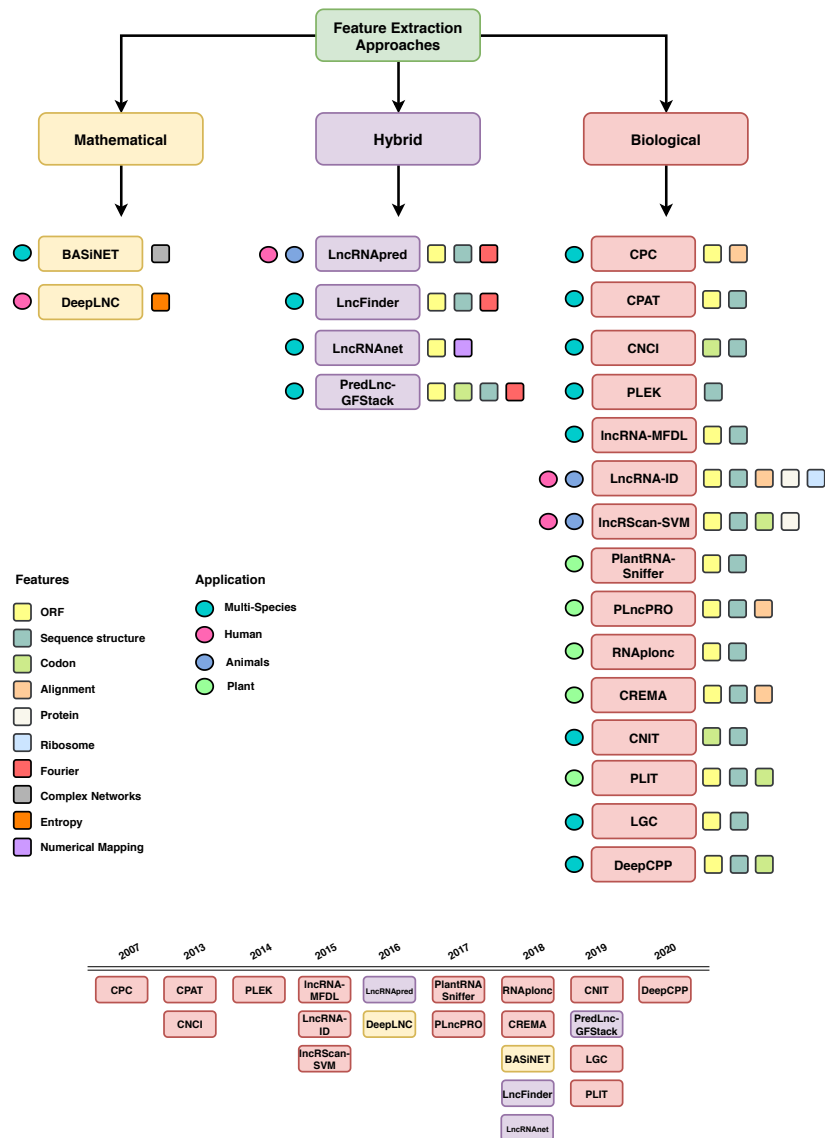


Figure 1: Feature extraction approaches in our case study divided into: Mathematical, Biological, and Hybrid.

141 score, total bit score, and frame entropy. RNAplonc classified sequences with
 142 the REPtree algorithm, considering 16 features (ORF, GC content, K-mer
 143 scheme ($k = 1, \dots, 6$), sequence length). BASiNET classifies sequences based
 144 on the feature extraction from complex network measurements. LncFinder

145 tests five classifiers (LR, SVM, RF, Extreme Learning Machine, and Deep
146 Learning), to apply the algorithm that obtains the highest accuracy. The
147 authors extract features from ORF, secondary structural, and EIIP-based
148 physicochemical properties.

149 CREMA uses ensemble machine learning classifiers. Features include
150 mRNA length, ORF (length), GC content, Fickett score, hexamer score,
151 alignment, transposable element, and sequence percent divergence from a
152 transposable element. LncRNAnet applies a deep learning-based approach
153 using numerical mapping and ORF indicators. CNIT is the updated CNCI
154 tool with a novel approach (XGBoost models with adjoining nucleotide triplets
155 and MLCDS). PLIT is a new alignment-free tool that uses ORF, transcript
156 length, Fickett score, Hexamer Score, GC content, and codon-bias features.

157 Lastly, PredLnc-GFStack also uses the stacked ensemble learning method
158 by extracting features based on codon-bias, Fickett score, ORF, GC content,
159 coding sequence, transcript length, k-mer, CTD, Hexamer score, signal to
160 noise ratio, UTR coverage, EDP of transcripts (entropy density profiles)
161 and structure-related. LGC proposes a feature relationship-based approach
162 (ORF length and GC content). DeepCPP is a deep learning method for
163 RNA coding potential prediction. Among the extracted features are ORF,
164 hexamer score, Fickett score, k-mer, g-gap, and nucleotide bias.

165 In general, the aforementioned works apply supervised learning methods
166 using binary classification (two classes - lncRNAs and protein-coding genes
167 (mRNA)). There is a considerable amount of research on humans, followed
168 by animals and plants. Regarding feature extraction, we observed a full do-
169 main of ORF and sequence-structure descriptors. As seen in Figure 1, there
170 is a frequent use of biological features. On the other hand, some works have
171 explored mathematical approaches for feature extraction, such as Genomic
172 Signal Processing (GSP), DNA Numerical Representation (DNR) [61, 26],
173 and Complex Networks [66]. Nevertheless, the authors used these charac-
174 teristics in conjunction with other biological feature extraction techniques
175 or without testing other mathematical features. Practically no papers have
176 focused on several mathematical approaches. Based on this, the objective of
177 this section was to summarize the main methods of the literature and their
178 characteristic descriptors. Therefore, we will not use the works shown for
179 comparison, but the most applied features.

180 3. Materials and Methods

181 In this section, we describe the methodological approach used to achieve
182 the proposed objectives, as shown in Figure 2. Essentially, we divided our
183 study into five stages: (1) Data selection and preprocessing; (2) Feature
184 extraction; (3) Training; (4) Testing; (5) Performance analysis. Hence, each
185 stage of the study is described, as well as information about the adopted
186 process.

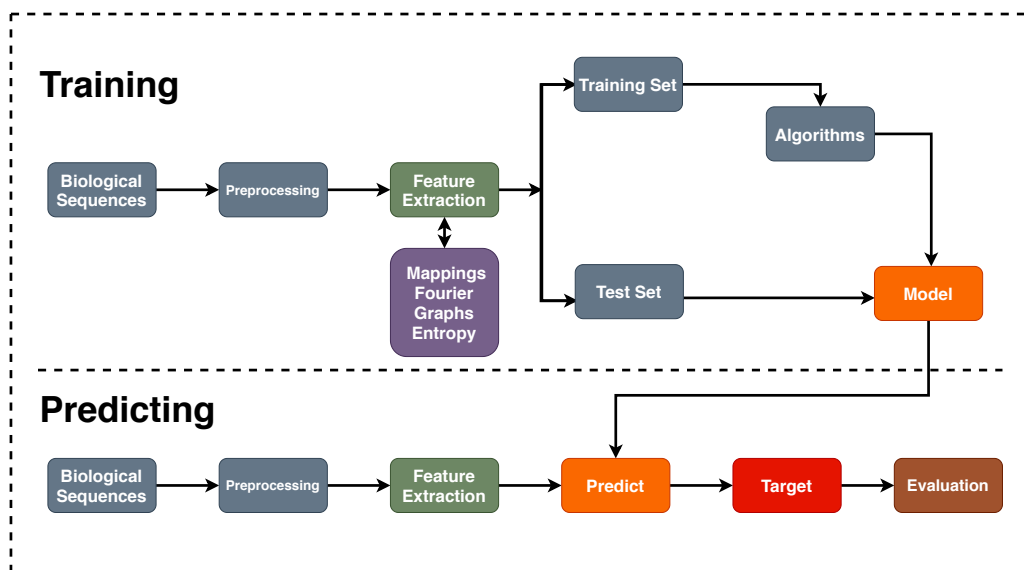


Figure 2: Proposed Pipeline. Essentially, (1) datasets are preprocessed; (2) Feature extraction techniques are applied to each dataset; (3) Machine learning algorithms are executed in the training set to induce predictive models; (4) Induced models are applied to the test set; Finally, (5) the models are evaluated.

187 This work was also divided into two case studies: (I) We assessed our
188 mathematical approaches with the most addressed problem in our review,
189 e.g., lncRNA vs. mRNA; (II) We tested its generalization on different clas-
190 sification problems.

191 3.1. Data Selection

192 As previously mentioned, we chose the lncRNAs classification problem,
193 because it is a new and relevant theme in the literature, in which, recently,
194 it has presented several works, mainly with ML, as explored in Section 2.

195 However, we will also adopt other datasets to assess the generalization of
196 mathematical features. As preprocessing, we used only sequences longer
197 than 200nt [57], and we also removed sequence redundancy. Moreover, the
198 sampling method was adopted in our dataset, since we are faced with the
199 *imbalanced data problem* [20]. Therefore, we applied random majority under-
200 sampling, which consists of removing samples from the majority class (to
201 adjust the class distribution) [74]. Finally, we divided this paper into two
202 case studies.

203 *3.1.1. Case Study I*

204 Sequences of five plant species were adopted to validate the proposed
205 approaches. The summary of the dataset can be seen in Table 1. According to
206 the literature approaches, this study also adopts two classes for the datasets:
207 the positive class, with lncRNAs, and the negative class, with protein-coding
208 genes (mRNAs).

Table 1: Adopted species to create the datasets.

Species	Sequences	Samples	Preprocessing	Selected
<i>A. trichopoda</i>	lncRNA	5698	4556	4556
	mRNA	26846	22326	4556
<i>A. thaliana</i>	lncRNA	2540	2540	2540
	mRNA	13973	13973	2540
<i>C. sinensis</i>	lncRNA	2562	2215	2215
	mRNA	46147	45846	2215
<i>C. sativus</i>	lncRNA	1929	1730	1730
	mRNA	30364	29829	1730
<i>R. communis</i>	lncRNA	4198	3487	3487
	mRNA	31221	29042	3487

209 The mRNA data of the *Arabidopsis thaliana* (obtained from CPC2 [25])
210 were built from the RefSeq database with protein sequences annotated by
211 Swiss-Prot [25], and lncRNA data from the Ensembl (v87) and Ensembl
212 Plants (v32) database. The mRNA transcript data of the *Amborella tri-*
213 *chopoda*, *Citrus sinensis*, *Cucumis sativus* and *Ricinus communis* were ex-
214 tracted from Phytozome (version 13) [75]. The lncRNAs data from these
215 species were extracted from GreeNC (version 1.12) [76].

216 *3.1.2. Case Study II*

217 In this case study, we will apply the best mathematical models (con-
218 sidering accuracy) of case study I to different classification problems with
219 lncRNAs, in order to test their generalization. Thus, divided this part into
220 three problems:

221 • **Problem 1** (lncRNA vs. sncRNA): Dataset with only non-coding
222 sequences (lncRNA and Small non-coding RNAs (sncRNAs), also ob-
223 tained from [25])

224 – lncRNA: 1291 sequences — sncRNA: 1291 sequences

225 • **Problem 2** (lncRNA vs. Antisense): Dataset with lncRNAs and long
226 noncoding antisense transcripts (obtained from [77]).

227 – lncRNA: 57 sequences — Antisense: 57 sequences

228 • **Problem 3** (circRNA vs. lncRNA): Dataset with lncRNA and circu-
229 lar RNAs (cirRNAs) sequences (circRNA obtained from PlantcircBase
230 [78]. This problem was based on [21] and [27], in order to classify
231 circRNA from other lncRNAs.

232 – circRNA: 2540 sequences — lncRNA: 2540 sequences

233 It is important to emphasize that we used only sequences from *Arabidop-*
234 *sis thaliana* in this second case study because it is the model species in
235 plants. Moreover, plant sequences is the least addressed field by the studies,
236 consequently presenting more challenges.

237 *3.2. Feature Extraction*

238 In this section, 9 feature extraction approaches are shown: 6 numer-
239 ical mapping techniques with Fourier transform, Entropy, Complex Net-
240 works. It is necessary to emphasize that we denote a biological sequence
241 $\mathbf{s} = (s[0], s[1], \dots, s[N - 1])$ such that $\mathbf{s} \in \{A, C, G, T\}^N$ [20].

242 *3.3. Fourier Transform and Numerical Mappings*

243 To extract features based on a Fourier model, we applied the Discrete
244 Fourier Transform (DFT), widely used for digital image and signal processing
245 (here GSP), which can reveal hidden periodicities after transformation of
246 time domain data to frequency domain space [79]. According to Yin and

²⁴⁷ Yau [80], the DFT of a signal with length N , $\mathbf{x} \in \mathbb{R}^N$, at frequency k , can
²⁴⁸ be defined by Equation (1):

$$X[k] = \sum_{n=0}^{N-1} x[n] e^{-j \frac{2\pi}{N} kn}, \quad k = 0, 1, \dots, N-1. \quad (1)$$

²⁴⁹ This method has been widely studied in bioinformatics, mainly for
²⁵⁰ analysis of periodicities and repetitive elements in DNA sequences [81] and
²⁵¹ protein structures [82]. This approach is shown in Figure 3 and was based
²⁵² on [20].

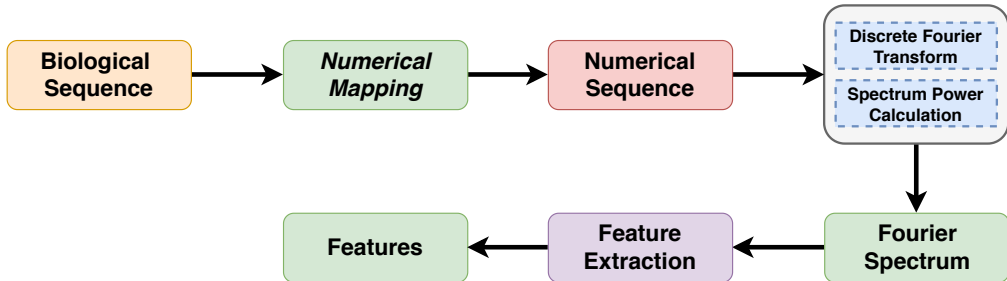


Figure 3: Fourier Transform and Numerical Mapping Pipeline. (1) Each sequence is mapped to a numerical sequence; (2) DFT is applied to the generated sequence; (3) The spectrum power is calculated; (4) The Feature Extraction is performed; Finally, (5) the features are generated.

²⁵³ To calculate DFT, we will use the Fast Fourier Transform (FFT), that
²⁵⁴ is a highly efficient procedure for computing the DFT of a time series [83].
²⁵⁵ However, to use GSP techniques, a numeric representation should be used
²⁵⁶ for the transformation or mapping of genomic data. In the literature, dis-
²⁵⁷ tinct DNR techniques have been developed [84]. According to Mendizabal-
²⁵⁸ Ruiz et al. [85], these representations can be divided into three categories:
²⁵⁹ single-value mapping, multidimensional sequence mapping, and cumulative
²⁶⁰ sequence mapping. Thereby, we study 6 numerical mapping techniques (or
²⁶¹ representations), which will be presented below: Voss [86], Integer [85, 87],
²⁶² Real [88], Z-curve [89], EIIP [90] and Complex Numbers [84, 91, 92].

²⁶³ 3.3.1. Voss Representation

²⁶⁴ This representation can use single or multidimensional vectors. Funda-
²⁶⁵ mentally, this approach transforms a sequence $\mathbf{s} \in \{A, C, G, T\}^N$ into a

266 matrix $\mathbf{V} \in \{0, 1\}^{4 \times N}$ such that $\mathbf{V} = [\mathbf{v}_1, \mathbf{v}_2, \mathbf{v}_3, \mathbf{v}_4]^T$, where T is the trans-
 267 pose operator and each \mathbf{v}_i array is constructed according to the following
 268 relation:

$$v_i[n] = \begin{cases} 1, & s[n] = \alpha[i] \\ 0, & s[n] \neq \alpha[i] \end{cases}, \text{ where } \alpha = (A, C, G, T), \quad n = 0, 1, \dots, N - 1. \quad (2)$$

269 As a result, each row of matrix \mathbf{V} may be seen as an array that marks each
 270 base position such that the first row denotes the presence of base A , row two
 271 for base C , row three base G and the last row for base T . For example, let $\mathbf{s} =$
 272 $(G, A, G, A, G, T, G, A, C, C, A)$ be a sequence that needs to be represented
 273 using Voss representation, therefore, $\mathbf{v}_1 = (0, 1, 0, 1, 0, 0, 0, 1, 0, 0, 1)$, which
 274 represents the locations of bases A , $\mathbf{v}_2 = (0, 0, 0, 0, 0, 0, 0, 0, 1, 1, 0)$ for bases
 275 C , $\mathbf{v}_3 = (1, 0, 1, 0, 1, 0, 1, 0, 0, 0, 0)$ for the G bases, $\mathbf{v}_4 = (0, 0, 0, 0, 0, 1, 0,$
 276 $0, 0, 0, 0)$ for T bases. Then, using the DFT in the indicator sequences shown
 277 above, we obtain (see Equation 3):

$$V_i[k] = \sum_{n=0}^{N-1} v_i[n] e^{-j \frac{2\pi}{N} kn}, \quad \forall i \in [1, 4], \quad k = 0, 1, \dots, N - 1. \quad (3)$$

278 The power spectrum of a biological sequence can be obtained by Equation
 279 (4):

$$P_V[k] = \sum_{i=1}^4 |V_i[k]|^2, \quad k = 0, 1, \dots, N - 1. \quad (4)$$

280 3.3.2. Integer Representation

281 This representation is one-dimensional [87, 85]. This mapping can be
 282 obtained by substituting the four nucleotides (T, C, A, G) of a biological
 283 sequence for integers (0, 1, 2, 3), respectively, e.g., let $\mathbf{s} = (G, A, G, A, G,$
 284 $T, G, A, C, C, A)$, thus, $\mathbf{d} = (3, 2, 3, 2, 3, 0, 3, 2, 1, 1, 2)$, as exposed in
 285 Equation (5). The DFT and power spectrum are presented in Equation (6).

$$d[n] = \begin{cases} 3, & s[n] = G \\ 2, & s[n] = A \\ 1, & s[n] = C \\ 0, & s[n] = T \end{cases}, \quad n = 0, 1, \dots, N - 1. \quad (5)$$

$$D[k] = \sum_{n=0}^{N-1} d[n] e^{-j \frac{2\pi}{N} kn}, \quad P_D[k] = |D[k]|^2, \quad k = 0, 1, \dots, N-1. \quad (6)$$

3.3.3. Real Representation

In this representation, Chakravarthy et al. [88] use real mapping based on the complement property of the complex mapping of [81]. This mapping applies negative decimal values for the purines (A, G), and positive decimal values for the pyrimidines (C, T), e.g., let $\mathbf{s} = (G, A, G, A, G, T, G, A, C, C, A)$, thus, $\mathbf{r} = (-0.5, -1.5, -0.5, -1.5, -0.5, 1.5, -0.5, -1.5, 0.5, 0.5, -1.5)$, as Equation (7) and Equation (8).

$$r[n] = \begin{cases} -0.5, & s[n] = G \\ -1.5, & s[n] = A \\ 0.5, & s[n] = C \\ 1.5, & s[n] = T \end{cases} \quad n = 0, 1, \dots, N-1. \quad (7)$$

293

$$R[k] = \sum_{n=0}^{N-1} r[n] e^{-j \frac{2\pi}{N} kn}, \quad P_R[k] = |R[k]|^2, \quad k = 0, 1, \dots, N-1. \quad (8)$$

3.3.4. Z-curve Representation

The Z-curve scheme is a three-dimensional curve presented by [89], to encode DNA sequences with more biological semantics. Essentially, we can inspect a given sequence $s[n]$ of length N , taking into account the n -th element of the sequence ($n = 1, 2, \dots, N$). Then, we denote the cumulative occurrence numbers A_n, C_n, G_n and T_n for each base A, C, G and T , as the number of times that a base occurred from $s[1]$ up until $s[n]$. Fundamentally, this method reduces the number of indicator sequences from four (Voss) to three (Z-curve) in a symmetrical way for all four components [93]. Therefore:

$$A_n + C_n + G_n + T_n = n \quad (9)$$

303 Where the Z-curve consists of a series of nodes P_1, P_2, \dots, P_N , whose
 304 coordinates $x[n], y[n]$, and $z[n]$ ($n = 1, 2, \dots, N$) are uniquely determined by
 305 the Z-transform, shown in Equation (10):

$$P[n] = \begin{cases} x[n] = (A_n + G_n) - (C_n + T_n) \\ y[n] = (A_n + C_n) - (G_n + T_n), \\ z[n] = (A_n + T_n) - (C_n + G_n) \end{cases} \quad (10)$$

$$x[n], y[n], z[n] \in [-n, n], \quad n = 1, 2, \dots, N.$$

306 The coordinates $x[n]$, $y[n]$, and $z[n]$ represent three independent distri-
 307 butions that fully describe a sequence [84]. Therefore, we will have three dis-
 308 tributions with definite biological significance: (1) $x[n]$ = purine/pyrimidine,
 309 (2) $y[n]$ = amino/keto, (3) $z[n]$ = weak hydrogen bonds/strong hydro-
 310 gen bonds [89], e.g., let $\mathbf{s} = (G, A, G, A, G, T, G, A, C, C, A)$, thus,
 311 $\mathbf{x} = (1, 2, 3, 4, 5, 4, 5, 6, 5, 4, 5)$; $\mathbf{y} = (-1, 0, -1, 0, -1, -2, -3, -2, -1, 0, 1)$;
 312 $\mathbf{z} = (-1, 0, -1, 0, -1, 0, -1, 0, -1, -2, -1)$. Essentially, the difference be-
 313 tween each dimension at the n -th position and the previous ($n - 1$) position
 314 can be either 1 or -1 [89]. Therefore, we may define the following set of
 315 equations in order to update the values of each dimension array considering
 316 that $x[-1] = y[-1] = z[-1] = 0$:

$$x[n] = \begin{cases} x[n-1] + 1, & s[n] = A \text{ or } G \\ x[n-1] - 1, & s[n] = C \text{ or } T \end{cases} \quad (11)$$

$$y[n] = \begin{cases} y[n-1] + 1, & s[n] = A \text{ or } C \\ y[n-1] - 1, & s[n] = G \text{ or } T \end{cases} \quad n = 1, 2, \dots, N. \quad (12)$$

$$z[n] = \begin{cases} z[n-1] + 1, & s[n] = A \text{ or } T \\ z[n-1] - 1, & s[n] = G \text{ or } C \end{cases} \quad (13)$$

317 Finally, the DFT and power spectrum may be defined as [94]:

$$X[k] = \sum_{n=1}^N x[n]e^{-j\frac{2\pi}{N}kn}, \quad Y[k] = \sum_{n=1}^N y[n]e^{-j\frac{2\pi}{N}kn}, \quad Z[k] = \sum_{n=1}^N z[n]e^{-j\frac{2\pi}{N}kn}. \quad (14)$$

$$P_C[k] = |X[k]|^2 + |Y[k]|^2 + |Z[k]|^2, \quad k = 1, 2, \dots, N. \quad (15)$$

318 3.3.5. EIIP Representation

319 Nair and Sreenadhan [90] proposed EIIP values of nucleotides to repre-
 320 sent biological sequences and to locate exons. According to the authors, a

321 numerical sequence representing the distribution of free electron energies can
 322 be called "*EIIP indicator sequence*", e.g., let $\mathbf{s} = (\text{G}, \text{A}, \text{G}, \text{A}, \text{G}, \text{T}, \text{G}, \text{A},$
 323 $\text{C}, \text{C}, \text{A})$, thus, $\mathbf{b} = (0.0806, 0.1260, 0.0806, 0.1260, 0.0806, 0.1335, 0.0806,$
 324 $0.1260, 0.1340, 0.1340, 0.1260)$, as shown in Equation (16). The DFT and
 325 power spectrum of this representation are presented in Equation (17).

$$b[n] = \begin{cases} 0.0806, & s[n] = G \\ 0.1260, & s[n] = A \\ 0.1340, & s[n] = C \\ 0.1335, & s[n] = T \end{cases} \quad n = 0, 1, \dots, N - 1. \quad (16)$$

$$B[k] = \sum_{n=0}^{N-1} b[n] e^{-j \frac{2\pi}{N} kn}, \quad P_B[k] = |B[k]|^2, \quad k = 0, 1, \dots, N - 1. \quad (17)$$

326 3.3.6. Complex Numbers Representation

327 This numerical mapping has the advantage of better translating some of
 328 the nucleotides features into mathematical properties [92] and represents the
 329 complementary nature of AT and CG pairs [84]; e.g., let $\mathbf{s} = (\text{G}, \text{A}, \text{G}, \text{A},$
 330 $\text{G}, \text{T}, \text{G}, \text{A}, \text{C}, \text{C}, \text{A})$, thus, $\bar{\mathbf{r}} = (-1 - j, 1 + j, -1 - j, 1 + j, -1 - j, 1 - j,$
 331 $-1 - j, 1 + j, -1 + j, -1 + j, 1 + j)$, as shown in Equation (18). The DFT
 332 and power spectrum of this representation are presented in Equation (19).

$$\bar{r}[n] = \begin{cases} -1 - j, & s[n] = G \\ 1 + j, & s[n] = A \\ -1 + j, & s[n] = C \\ 1 - j, & s[n] = T \end{cases} \quad n = 0, 1, \dots, N - 1. \quad (18)$$

$$\bar{R}[k] = \sum_{n=0}^{N-1} \bar{r}[n] e^{-j \frac{2\pi}{N} kn}, \quad P_{\bar{R}}[k] = |\bar{R}[k]|^2, \quad k = 0, 1, \dots, N - 1. \quad (19)$$

333 3.3.7. Features

334 The feature extraction is applied in each representation with Fourier
 335 transform, adopting Peak to Average Power Ratio (PAPR), mistakenly con-
 336 fused with the Signal to Noise Ratio (SNR), average power spectrum, me-
 337 dian, maximum, minimum, sample standard deviation, population standard
 338 deviation, percentile (15/25/50/75), amplitude, variance, interquartile range,

339 semi-interquartile range, coefficient of variation, skewness, and kurtosis. Ac-
 340 cording to [95], the RNA has a statistical phenomenon known as period-3
 341 behavior or 3-base periodicity, where the peak power will always be at the
 342 sample $N/3$. The PAPR is defined as [96]:

$$PAPR = \frac{\max_{0 \leq k \leq N-1} (P[k])}{\frac{1}{N} \sum_{k=0}^{N-1} P[k]} \quad (20)$$

343 3.4. Entropy

344 Information theory has been widely used in bioinformatics [97, 98]. Based
 345 on this, we consider the study of [99], which applied an algorithmic and
 346 mathematical approach to DNA code analysis using entropy and phase plane.
 347 According to [98], entropy is a measure of the uncertainty associated with a
 348 probabilistic experiment. To generate a probabilistic experiment, we use a
 349 known approach in bioinformatics, the k-mer (our pipeline - Figure 4).

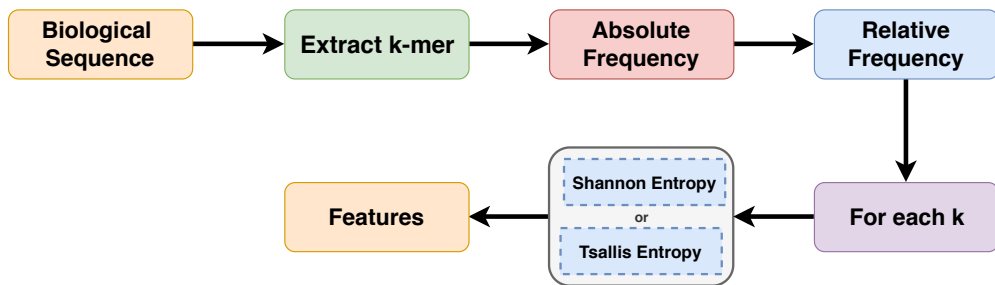


Figure 4: Entropy Pipeline. (1) Each sequence is mapped in k -mers; (2) The absolute frequency of each k is calculated; (3) Based on absolute frequency, the relative frequency is calculated; (4) The Tsallis or Shannon entropy is applied to each k .

350 In this method, each sequence is mapped in the frequency of neighboring
 351 bases k , generating statistical information. The k -mer is denoted by P_k ,
 352 corresponding to Equation (21).

$$P_k(\mathbf{s}) = \frac{c_i^k}{N - k + 1} = \left(\frac{c_1^1}{N - 1 + 1}, \dots, \frac{c_4^1}{N - 1 + 1}, \right. \\ \left. \frac{c_{4+1}^2}{N - 2 + 1}, \dots, \frac{c_i^k}{N - k + 1} \right) \quad k = 1, 2, \dots, 24. \quad (21)$$

353 We applied this equation to each sequence with frequencies of $k = 1, 2,$
 354 $\dots, 24$. Where, c_i^k is the number of substring occurrences with length k in a
 355 sequence (\mathbf{s}) with length N , in which the index $i \in \{1, 2, \dots, 4^1 + \dots + 4^k\}$
 356 represents the analyzed substring. For a better understanding, Figure 5
 357 demonstrated an example with $k = 6$ and $k = 9$.

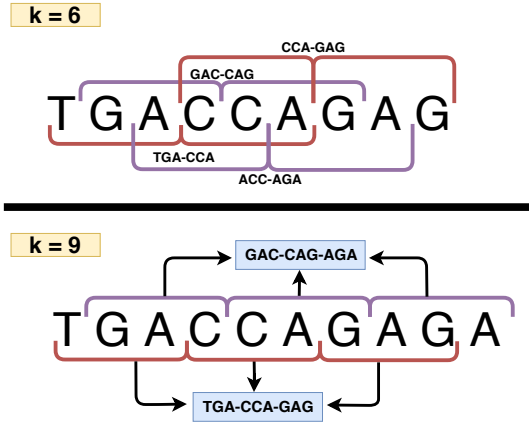


Figure 5: k -mer Workflow. Example with $k = 6$ and $k = 9$.

358 Basically, histograms with short bins are adopted, such as $[\{A\}, \{C\},$
 359 $\{G\}, \{T\}]$, that occur for $k = 1$, up to histograms with long sequence count-
 360 ing bins such as $[\{GGGGGGGGGGGGG\}, \dots, \{AAAAAAAAAAAA\}]$, that
 361 result for $k = 12$. Where, after counting the absolute frequencies of each k ,
 362 we generate relative frequencies (see Equation (21)), and then apply Shannon
 363 and Tsallis entropy to generate the features.

364 3.4.1. Shannon and Tsallis Entropy

365 Fundamentally, we chose Shannon entropy, because it quantifies the amount
 366 of information in a variable [100], that is, we can reach a single value that
 367 quantifies the information contained in different observation periods (e.g.,
 368 our case: k-mer). However, according to [101], it is important to explore a
 369 generalized form of the Shannon's entropy. Based on this, we have opted for
 370 a generalized entropy proposed by Tsallis, applied by several works in the lit-
 371 erature [102, 103]. Thereby, for a discrete random variable F taking values in
 372 $\{f[0], f[1], f[2], \dots, f[N-1]\}$ with probabilities $\{p[0], p[1], p[2], \dots, p[N-1]\}$,
 373 represented as $P(F = f[n]) = p[n]$. The Shannon (Equation 22) and Tsallis
 374 (Equation 23) entropy associated with this variable is given by the following
 375 expressions:

$$H_S[k] = - \sum_{n=0}^{N-1} p_k[n] \log_2 p_k[n] \quad k = 1, 2, \dots, 24. \quad (22)$$

$$H_T[k] = \frac{1}{q-1} \left(1 - \sum_{n=0}^{N-1} p_k[n]^q \right) \quad k = 1, 2, \dots, 24. \quad (23)$$

376 Where k represents the analyzed k -mer, N the number of possible events
 377 and $p[n]$ the probability that event n occurs.

378 *3.5. Complex Networks*

379 Complex networks are widely used in mathematical modeling and have
 380 been an extremely active field in recent years [104], as well as becoming an
 381 ideal research area for mathematicians, computer scientists, and biologists.
 382 Based on this, we consider the study of [66], in which we propose a feature
 383 extraction model based on complex networks, as shown in Figure 6.

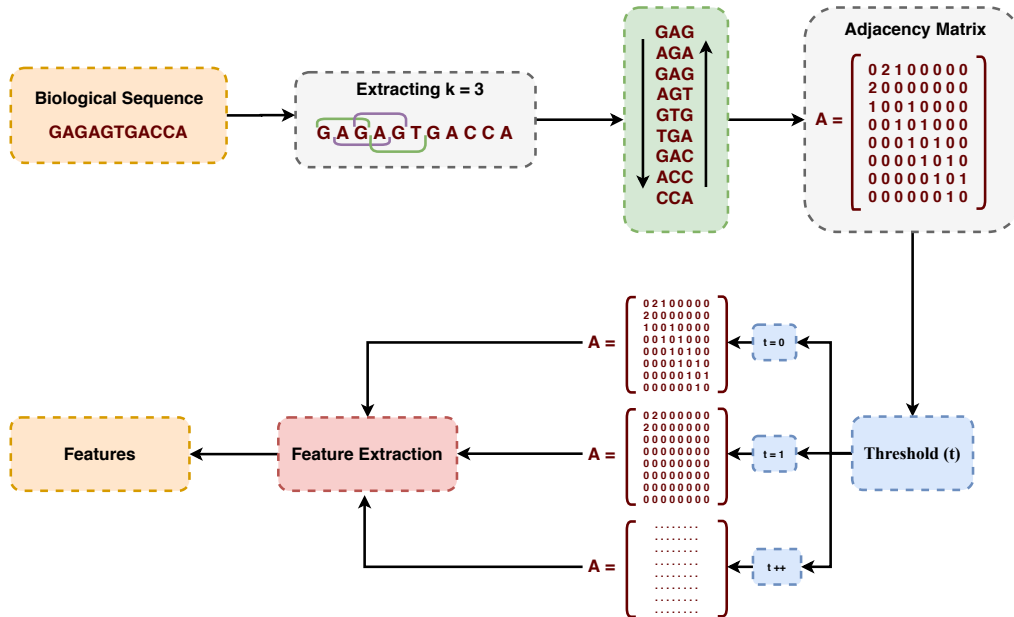


Figure 6: Complex Networks Pipeline. (1) Each sequence is mapped in the frequency of neighboring bases k ($k = 3$); (2) This mapping is converted to a undirected graph represented by an adjacency matrix; (3) Feature extraction is performed using a threshold scheme; Finally, (4) the features are generated.

384 Each sequence is mapped to the frequency of neighboring bases k ($k =$
385 3 - see Figure 5). This mapping is converted into an undirected graph rep-
386 resented by an adjacency matrix, in which we applied a threshold scheme
387 for feature extraction, thus generating our characteristic vector. Fundamen-
388 tally, we represent our structure by undirected weighted graphs. According
389 to [104], a graph $G = \{V, E\}$ is structured by a set V of vertices (or nodes)
390 connected by a set E of edges (or links). Each edge reflects a link between
391 two vertices, e.g., $e_p = (i, j)$ connection between the vertices i and j [104].
392 If there is an edge connecting the vertices i and j , the elements a_{ij} are equal
393 to 1, and equal to 0 otherwise.

394 In our case, the graph is undirected, that is, the adjacency matrix A
395 is symmetric, e.g., elements $a_{ij} = a_{ji}$ for any i and j [104]. Furthermore,
396 we apply a threshold scheme presented by [66], in which we extract weight
397 of the edges to capture adjacencies at different frequencies. Finally, as fea-
398 tures, several network characterization measures were obtained, based on
399 [66, 105], among them: Betweenness, assortativity, average degree, average
400 path length, minimum degree, maximum degree, degree standard deviation,
401 frequency of motifs (size 3 and 4), clustering coefficient.

402 *3.6. Normalization, Training and Evaluation Metrics*

403 Data normalization is a preprocessing technique often applied to a dataset.
404 Essentially, features can have different dynamic ranges. This problem may
405 have a stronger effect in the induction of a predictive model, mainly for
406 distance-based ML algorithms. Consequently, the application of a normal-
407 ization procedure makes the ranges similar, reducing this problem [106]. We
408 used the min-max normalization, which reduces the data range to 0 and 1
409 (or -1 to 1, if there are negative values) [20]. The general formula is given as
410 (Equation (24)) [107]:

$$x'_{ij} = \frac{x_{ij} - \min(j)}{\max(j) - \min(j)}. \quad (24)$$

411 Where x is the original value and x'_{ij} is its normalized version. Further-
412 more, $\min(j)$ and $\max(j)$ are, respectively, the smallest and largest values of
413 a feature j [6, 107]. Next, we investigate three classification algorithms, such
414 as Random Forest (RF) [108], AdaBoost [109] and CatBoost [110]. We chose
415 these ML algorithms because they induce interpretable predictive models
416 when humans can easily understand the internal decision-making process.
417 Thus, domain experts can validate the knowledge used by the models for

418 the classification of new sequences [6]. Finally, to induce our models, we
 419 used 70% of samples for *training* (with 10-fold cross-validation) and 30% for
 420 *testing*, as shown in Table 2.

Table 2: Number of sequences used for training and testing in each dataset.

Case Study	Dataset	Samples	Training	Testing
I	<i>A. trichopoda</i>	9112	6378	2734
	<i>A. thaliana</i>	5080	3556	1524
	<i>C. sinensis</i>	4430	3101	1329
	<i>C. sativus</i>	3460	2422	1038
	<i>R. communis</i>	6974	4881	2093
II	<i>lncRNA vs. sncRNA</i>	2582	1807	775
	<i>lncRNA vs. Antisense</i>	114	79	35
	<i>circRNA vs. lncRNA</i>	5080	3556	1524

421 The methods were evaluated with four measures: Sensitivity (SE - Equa-
 422 tion 26), Specificity (SPC - Equation 27), Accuracy (ACC - Equation 25),
 423 and Cohen's kappa coefficient [111] (Equation 28).

$$ACC = \frac{TP + TN}{TN + FP + TP + FN} \quad SPC = \frac{TN}{TN + FP} \quad (27)$$

$$SE = \frac{TP}{TP + FN} \quad (26) \quad Kappa = \frac{p_o - p_e}{1 - p_e} \quad (28)$$

424 These measures use True Positive (TP), True Negative (TN), False Posi-
 425 tive (FP) and False Negative (FN) values, where: TP measures the correctly
 426 predicted positive label; TN represents the correctly classified negative label;
 427 FP describes all those negative entities that are incorrectly classified as pos-
 428 itive and; FN represents the positive label that are incorrectly classified as
 429 the negative label.

430 4. Results

431 This section shows experimental results from 9 feature extraction ap-
 432 proaches with mathematical models for biological sequences, divided into
 433 two parts: Case Study I and Case Study II.

434 *4.1. Case Study I*

435 Initially, we induced models with the RF, AdaBoost, and CatBoost clas-
 436 sifiers in the training set of three datasets (*A. trichopoda*, *A. thaliana*, and *R.*
 437 *communis*, we randomly chose three datasets for evaluating the classifiers).
 438 Our initial goal is to choose the best classifier to follow in the testing phases.
 439 Thereby, to estimate the real accuracy, we applied 10-fold cross-validation,
 440 as shown in Table 3.

Table 3: Accuracy for the training set (*A. trichopoda*, *A. thaliana*, and *R. communis*) using 10-fold cross-validation.

Dataset	Model	RF	AdaBoost	CatBoost
<i>A. trichopoda</i>	Z-curve	0.90 (\pm 0.03)	0.91 (\pm 0.02)	0.92 (\pm 0.02)
	Binary	0.92 (\pm 0.02)	0.94 (\pm 0.02)	0.94 (\pm 0.02)
	Real	0.91 (\pm 0.02)	0.93 (\pm 0.02)	0.94 (\pm 0.02)
	Integer	0.91 (\pm 0.02)	0.93 (\pm 0.02)	0.94 (\pm 0.02)
	EIIP	0.92 (\pm 0.02)	0.94 (\pm 0.02)	0.94 (\pm 0.02)
	Complex	0.92 (\pm 0.03)	0.94 (\pm 0.02)	0.94 (\pm 0.02)
	Graphs	0.92 (\pm 0.02)	0.94 (\pm 0.02)	0.94 (\pm 0.02)
	Shannon	0.92 (\pm 0.02)	0.94 (\pm 0.02)	0.94 (\pm 0.02)
	Tsallis	0.92 (\pm 0.02)	0.94 (\pm 0.02)	0.94 (\pm 0.02)
<i>A. thaliana</i>	Z-curve	0.95 (\pm 0.02)	0.93 (\pm 0.03)	0.94 (\pm 0.02)
	Binary	0.94 (\pm 0.02)	0.94 (\pm 0.02)	0.94 (\pm 0.02)
	Real	0.95 (\pm 0.02)	0.94 (\pm 0.02)	0.95 (\pm 0.02)
	Integer	0.94 (\pm 0.02)	0.94 (\pm 0.02)	0.94 (\pm 0.02)
	EIIP	0.95 (\pm 0.02)	0.94 (\pm 0.02)	0.95 (\pm 0.03)
	Complex	0.94 (\pm 0.02)	0.94 (\pm 0.02)	0.94 (\pm 0.01)
	Graphs	0.94 (\pm 0.02)	0.94 (\pm 0.02)	0.95 (\pm 0.02)
	Shannon	0.94 (\pm 0.02)	0.94 (\pm 0.02)	0.95 (\pm 0.02)
	Tsallis	0.94 (\pm 0.02)	0.94 (\pm 0.02)	0.94 (\pm 0.02)
<i>R. communis</i>	Z-curve	0.93 (\pm 0.02)	0.92 (\pm 0.02)	0.93 (\pm 0.02)
	Binary	0.95 (\pm 0.01)	0.95 (\pm 0.02)	0.95 (\pm 0.02)
	Real	0.95 (\pm 0.02)	0.94 (\pm 0.02)	0.94 (\pm 0.02)
	Integer	0.94 (\pm 0.01)	0.94 (\pm 0.01)	0.94 (\pm 0.02)
	EIIP	0.95 (\pm 0.02)	0.95 (\pm 0.02)	0.95 (\pm 0.01)
	Complex	0.95 (\pm 0.02)	0.95 (\pm 0.01)	0.95 (\pm 0.01)
	Graphs	0.95 (\pm 0.01)	0.95 (\pm 0.01)	0.95 (\pm 0.02)
	Shannon	0.95 (\pm 0.02)	0.95 (\pm 0.02)	0.95 (\pm 0.01)

	Tsallis	0.95 (± 0.01)	0.95 (± 0.01)	0.95 (± 0.01)
--	---------	----------------------	----------------------	----------------------

441 Assessing each classifier, we noted that the best performance was of the
 442 CatBoost with all mathematical models in *A. trichopoda*, followed by Ad-
 443 aBoost (6 best results) and RF (no better results). In *A. thaliana*, CatBoost
 444 kept the best performance (7 best results), followed by RF (6 best results)
 445 and AdaBoost (3 best results). In contrast, the RF classifier obtained the
 446 best results (6) in *R. communis*, followed by CatBoost (5 best results) and
 447 AdaBoost (3 best results). Based on this, we continued testing the models
 448 with the CatBoost classifier. Thus, in Table 4, we present the results of all
 449 mathematical models using 4 evaluation metrics.

Table 4: Performance analysis. This table compares the sensitivity, specificity, accuracy and kappa metrics for each model in the test sets using CatBoost classifier.

Dataset	Model	SE	SPC	ACC	Kappa
<i>A. trichopoda</i>	Z-curve	0.9744	0.8566	0.9155	0.8310
	Binary	0.9795	0.9005	0.9400	0.8800
	Real	0.9802	0.8837	0.9320	0.8639
	Integer	0.9773	0.8822	0.9298	0.8595
	EIIP	0.9781	0.8990	0.9386	0.8771
	Complex	0.9802	0.9012	0.9407	0.8815
	Graphs	0.9737	0.9020	0.9378	0.8756
	Shannon	0.9781	0.9020	0.9400	0.8800
	Tsallis	0.9795	0.9005	0.9400	0.8800
<i>A. thaliana</i>	Z-curve	0.9777	0.9383	0.9580	0.9160
	Binary	0.9619	0.9449	0.9534	0.9068
	Real	0.9803	0.9409	0.9606	0.9213
	Integer	0.9698	0.9436	0.9567	0.9134
	EIIP	0.9646	0.9449	0.9547	0.9094
	Complex	0.9724	0.9409	0.9567	0.9134
	Graphs	0.9685	0.9423	0.9554	0.9108
	Shannon	0.9738	0.9462	0.9600	0.9200
	Tsallis	0.9764	0.9409	0.9587	0.9173
<i>R. communis</i>	Z-curve	0.9021	0.8707	0.8864	0.7728
	Binary	0.8901	0.8707	0.8804	0.7607
	Real	0.9142	0.8571	0.8856	0.7713

<i>C. sinensis</i>	Integer	0.8825	0.8692	0.8758	0.7517
	EIIP	0.8840	0.8526	0.8683	0.7367
	Complex	0.9081	0.8496	0.8789	0.7577
	Graphs	0.9006	0.8632	0.8819	0.7637
	Shannon	0.9172	0.8586	0.8879	0.7758
	Tsallis	0.9262	0.8541	0.8901	0.7803
<i>C. sativus</i>	Z-curve	0.8979	0.8478	0.8728	0.7457
	Binary	0.9056	0.8459	0.8757	0.7514
	Real	0.9268	0.8439	0.8854	0.7707
	Integer	0.9056	0.8536	0.8796	0.7592
	EIIP	0.8979	0.8459	0.8719	0.7437
	Complex	0.9326	0.8343	0.8834	0.7669
	Graphs	0.9075	0.8536	0.8805	0.7611
	Shannon	0.9326	0.8382	0.8854	0.7707
<i>R. communis</i>	Tsallis	0.9403	0.8401	0.8902	0.7803
	Z-curve	0.9446	0.9140	0.9293	0.8586
	Binary	0.9417	0.9589	0.9503	0.9006
	Real	0.9589	0.9408	0.9498	0.8997
	Integer	0.9465	0.9456	0.9460	0.8920
	EIIP	0.9455	0.9551	0.9503	0.9006
	Complex	0.9398	0.9561	0.9479	0.8958
	Graphs	0.9455	0.9542	0.9498	0.8997
	Shannon	0.9388	0.9589	0.9489	0.8978
	Tsallis	0.9417	0.9608	0.9513	0.9025

As can be seen, all models presented robust results, with the worst performance (ACC) of 0.8901 (*C. sinensis*) and the best of 0.9606 (*A. thaliana*). That is, all models were robust in different datasets without a high loss of performance. Assessing each metric individually, we realized that in SE, the best performance was from Real representation (3 datasets), followed by Tsallis (2 datasets) and Complex numbers (1 dataset). In SPC, the best results were from Entropy (3 datasets), followed by Graphs (2 datasets). In ACC, Tsallis presented the best performance (3 datasets), followed by Real representation and Complex numbers (1 dataset). For each dataset, we can see in *A. trichopoda* the best ACC was 0.9407 (Complex); *A. thaliana* with 0.9606 (Real); *C. sinensis* with 0.8901 (Tsallis); *C. sativus* with 0.8902 (Tsallis); and *R. communis* with 0.9513 (Tsallis). Highlight for Tsallis entropy, which presented the best results, mainly in accuracy, proving to be more

463 generalist in the case study I.

464 *4.2. Case Study II*

465 After evaluating all methods in 5 datasets (lncRNA of different species)
466 and observing their results, we applied a second case study, where we used
467 only three mathematical models for generalization analysis, including GSP
468 (Fourier + complex numbers), entropy (Tsallis) and graphs (complex net-
469 works). Here, our objective was to analyze how each model (feature extrac-
470 tion approach) behaved in different biological sequence classification pro-
471 blems. In other words, we assessed the generalization of each approach to
472 classifying sequences with different structures (distinct problem). For this,
473 we tested 3 new datasets established in Section 3.1.2, as can be seen in Figure
474 7.

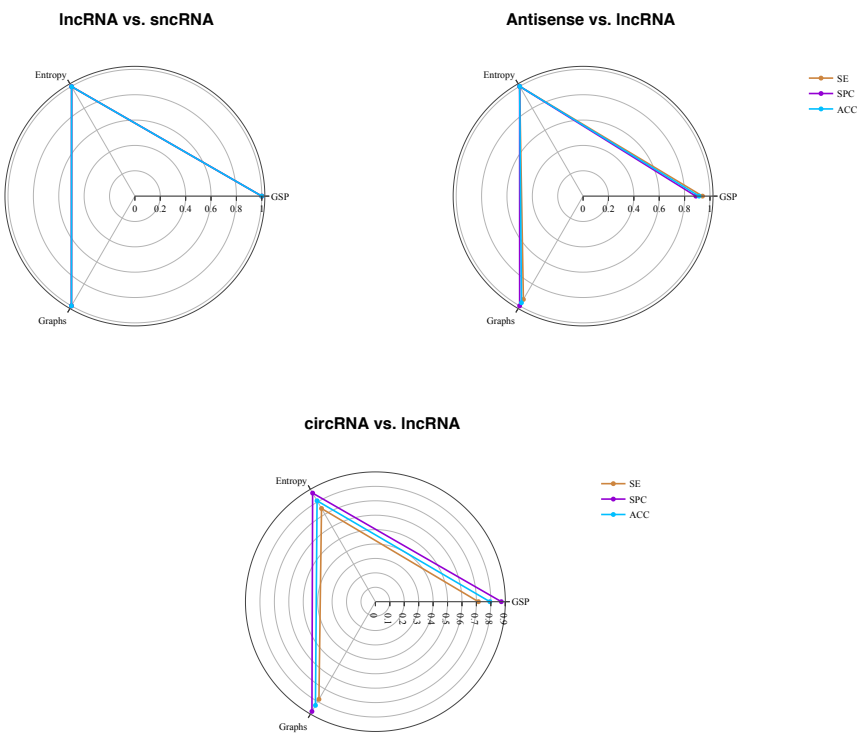


Figure 7: Performance analysis of three mathematical models, GSP (fourier + complex numbers), entropy (Tsallis) and graphs (complex networks), for different problems.

475 Again, all showed robust results, in which, graph-based models are the
476 best in 2 of the 3 problems analyzed, followed by entropy and GSP. In the
477 three datasets, our approaches have achieved relevant results with ACC, SE
478 and SPC, proving to be efficient and generalist, when exposed to different
479 problem scenarios. Furthermore, if we analyze at the last problem (circRNA
480 vs. lncRNA), our approaches were effective when compared to our references
481 that reached an ACC of 0.7780 [21] and 0.7890 [27] in their datasets against
482 0.8307 from our best model (graph - using these comparisons as an (indirect)
483 reference indicator).

484 *4.3. Statistical Significance Tests*

485 The statistical significance was assessed in both case studies (difference
486 in ACC), using Friedman's statistical test and the Conover post-hoc test.
487 Thereby, our null hypothesis ($H_0 = M(1) = M(2) = \dots = M(k)$), is tested
488 against the alternative hypothesis ($H_A = \text{at least one model has statistical}$
489 $\text{significance } (\alpha = 0.05, p < \alpha)$). First, we apply the global test in the case
490 study I, in which the Friedman test indicates significance ($\chi^2(8) = 17.34, p-$
491 value = 0.0268), that is, we can reject H_0 , as $p < 0.05$. Thus, it is essential to
492 execute the post-hoc statistical test. Conover statistics values were obtained,
493 as well as p -values (see Table 5), using 95% of significance ($\alpha = 0.05$).

Table 5: Conover statistics values - The accepted alternative hypothesis is in bold (p -values for $\alpha = 0.05$).

	Z-curve	Binary	Real	Integer	EIIP	Complex	Graphs	Shannon
Binary	0.5580	-	-	-	-	-	-	-
Real	0.1416	0.3671	-	-	-	-	-	-
Integer	0.7896	0.3956	0.0852	-	-	-	-	-
EIIP	0.9574	0.5230	0.1284	0.8309	-	-	-	-
Complex	0.3671	0.7489	0.5580	0.2451	0.3399	-	-	-
Graphs	0.5580	1.0000	0.3671	0.3956	0.5230	0.7489	-	-
Shannon	0.0687	0.2057	0.7089	0.0390	0.0616	0.3399	0.2057	-
Tsallis	0.0146	0.0550	0.2898	0.0075	0.0128	0.1050	0.0550	0.4892

494 Concerning to the Conover post-hoc test, entropy-based models have
495 highly significant differences for the Z-curve ($p < 0.0146$), Integer ($p < 0.0075$
496 - Tsallis and $p < 0.0390$ - Shannon), and EIIP ($p < 0.0128$). Possibly,
497 these results indicate that entropy has a more significant performance when
498 compared to representations with Fourier. However, other mathematical
499 models in case study I do not differ significantly, indicating their efficiency

500 in all datasets. Now, evaluating case study II, we realized that the global
501 test with Friedman's statistical test is not significant, in which we obtained
502 $\chi^2(2) = 1.64$, $p\text{-value} = 0.4412$, indicating that the three studied feature ex-
503 traction techniques show a similar performance in the problems, once more
504 confirming the effectiveness and robustness of all mathematical models.

505 *4.4. Computational Time*

506 In addition, we also assessed the computational time cost of each tested
507 model. To do this, we ran three models, GSP (Fourier + complex numbers),
508 entropy (Tsallis) and graphs (complex networks)), in 1291 random sequences,
509 as shown in Figure 8.

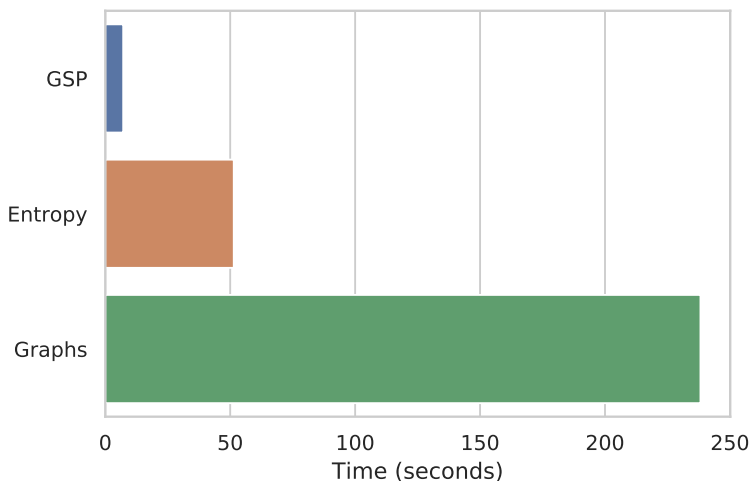


Figure 8: Execution Time.

510 We performed the experiments using Intel Core i3-9100F CPU (3.60GHz),
511 16GB memory, and running in Debian GNU/Linux 10. The lowest cost in
512 computational time is for models based on GSP (0m7.183s) and entropy
513 (0m51.427s), while graphs (3m58.208s) have a much higher cost. These re-
514 sults demonstrated that, although the models present a similar performance,
515 the computational time efficiency is significantly different.

516 5. Discussion

517 This section discusses our findings in terms of whether they support our
518 hypothesis (*feature extraction approaches based on mathematical models are*
519 *as efficient and generalist as biological approaches*). Overall, several exper-
520 imental tests were assumed in this research, in which all feature extraction
521 approaches based on mathematical models showed excellent results, as can
522 be seen in Table 4 and Figure 7. Regarding its performance in distinct clas-
523 sification problems, case study II, we used only three mathematical models
524 for generalization analysis, including GSP (Fourier + complex numbers), en-
525 tropy (Tsallis) and graphs (complex networks). In which, entropy and graph-
526 based models reported the best performance followed by GSP. Furthermore,
527 all models maintained robust results in different sequence classification prob-
528 lems.

529 Furthermore, to fully support our hypothesis, we also compare three
530 mathematical models shown in Figure 7 concerning a biological and hybrid
531 approach, in four datasets ((lncRNA vs. mRNA (case study I)); (lncRNA vs.
532 sncRNA; lncRNA vs. Antisense; circRNA vs. lncRNA (case study II)). Thus,
533 we generate our biological model using some of the most applied features in
534 Figure 1. Thus, features used by the models are:

- 535 • **Biological:** The features were provided by [25]: Fickett TESTCODE
536 score, isoelectric point, open reading frame (ORF) length, and ORF
537 integrity.
- 538 • **Hybrid:** The features were generated by one of the most current ap-
539 proaches in the literature (lncFinder [26] - 2018). We classify this model
540 as a hybrid because it uses a combination of biological and mathemati-
541 cal features. Among the biological characteristics is Logarithm-distance
542 of hexamer on ORF, length and coverage of the longest ORF. Regard-
543 ing mathematical features, [26] uses an EIIP-based physicochemical
544 property with Fourier Transform (similar to our approach with GSP,
545 but using only EIIP mapping).

546 For a fair comparison, the new experiments follow the same methodology
547 (70% training, 30% test, and CatBoost classifier), as shown in Table 6.

548 As can be seen, the hybrid model (0.9915) reported the best performance
549 in the first dataset (lncRNA vs. mRNA), followed by the biological (0.9816)
550 and our mathematical model (Entropy - 0.9587), with only a difference of

Table 6: Performance analysis of three mathematical models against a biological and hybrid model for different sequence classification problems.

lncRNA vs. mRNA				lncRNA vs. sncRNA			
Models	SE	SPC	ACC	Models	SE	SPC	ACC
GSP	0.9724	0.9409	0.9567	GSP	1.0000	1.0000	1.0000
Entropy	0.9764	0.9409	0.9587	Entropy	0.9974	0.9974	0.9974
Graphs	0.9685	0.9423	0.9554	Graphs	1.0000	1.0000	1.0000
Biological	0.9869	0.9764	0.9816	Biological	0.7855	0.8273	0.8065
Hybrid	0.9895	0.9934	0.9915	Hybrid	0.9509	0.9485	0.9497

lncRNA vs. Antisense				circRNA vs. lncRNA			
Models	SE	SPC	ACC	Models	SE	SPC	ACC
GSP	0.9412	0.8889	0.9143	GSP	0.7139	0.8727	0.7933
Entropy	1.0000	1.0000	1.0000	Entropy	0.7467	0.8701	0.8084
Graphs	0.9412	1.0000	0.9714	Graphs	0.7822	0.8793	0.8307
Biological	0.8889	0.9412	0.9143	Biological	0.6024	0.7612	0.6818
Hybrid	0.9412	0.7778	0.8571	Hybrid	0.7283	0.8819	0.8051

0.0328 and 0.0229, respectively. However, it is relevant to highlight that the biological and hybrid models use the ORF descriptor, a highly employed feature for discovering coding sequences and which, according to [19] is an essential guideline for distinguishing lncRNAs from mRNA. In other words, this explains the great result, but, as mentioned at the beginning of this manuscript, this type of feature with a biological insight is often difficult to reuse or adapt to another specific problem. Thereby, our study has a gain in terms of generalization, since this would not be possible only with the ORF. If we analyze at the hybrid model, in this first dataset, the gain was minimal compared to the biological (0.0099), confirming the efficiency of the previously mentioned features (ORF). This is different from our approaches, which showed an robust result without using bias features for the analyzed problem.

Hence, this hypothesis is proven in the other three datasets, where our mathematical models perform much better than the biological model, mainly in the fourth dataset (circRNA vs. lncRNA), in which we obtained a gain of 0.1489 in ACC. Regarding the hybrid model, it can be observed that the mixture of biological and mathematical characteristics helped to keep the

569 model competitive in all datasets, indicating the effectiveness of mathematical
570 features. Even so, our models showed the best results in three of the four
571 proposed problems. Therefore, our pipeline is efficient in terms of generalization
572 to classify lncRNA from mRNA, as well as other biological sequence
573 classification problems. We also assessed the statistical significance of the
574 mathematical versus biological approach in the previously applied tests, in
575 which entropy ($p < 0.0480$) and graphs ($p < 0.0200$) indicated significant results
576 concerning the biological model. Lastly, considering all these findings,
577 we fully support the suggested hypothesis.

578 6. Conclusion

579 This work proposed to analyze feature extraction approaches for biological
580 sequence classification. Specifically, we concentrated our work on the
581 study of feature extraction techniques using mathematical models. We ana-
582 lyzed mathematical models to propose efficient and generalist techniques for
583 different problems. As a case study, we used lncRNA sequences. Moreover,
584 we divided this paper into two case studies. In our experiments, as a start-
585 ing point, 9 mathematical models for feature extraction were analyzed: 6
586 numerical mapping techniques with Fourier transform; Tsallis and Shannon
587 entropy; Graphs (complex networks). Thereby, several biological sequence
588 classification problems were adopted to validate the proposed approach.

589 In our experiments, all mathematical models presented relevant and ro-
590 bust results, with performances (ACC) between 0.8901-0.9606 in case study I.
591 In case study II, once more, all showed effective results with models based on
592 entropy and graphs showing the best performance, followed by GSP. Further-
593 more, to validate our study, we compared three mathematical models against
594 a biological and hybrid approach, in four different datasets. In which, our
595 models demonstrated suitable results, and was superior or competitive and
596 robust in terms of generalization. Moreover, we verified that mathematical
597 approaches perform as accurately as biological approaches and have a better
598 generalization capacity since they outperform biological features in scenarios
599 not designed for them. Finally, among the different feature extraction ap-
600 proaches tested in this work, the combination of k-mer and entropy, as well
601 as complex networks performs better than GSP at the cost of a significant
602 increase in computational complexity.

603 **Declaration of Competing interests**

604 All authors declare that they have no conflict of interest.

605 **Financial support**

606 This project has been supported by a master scholarship from Federal
607 University of Technology - Paraná (UTFPR) (Grant: April/2018), CAPES
608 (April/2019 and PROEX-11919694/D), and PROBAL (Grant: CAPES/DAAD
609 - 88887.144045/2017-00).

610 **Acknowledgements**

611 The authors would like to thank UTFPR-CP, ICMC-USP, and CAPES
612 for the financial support given to this research.

References

- [1] H. Lou, M. Schwartz, J. Bruck, F. Farnoud, Evolution of k-mer frequencies and entropy in duplication and substitution mutation systems, IEEE Transactions on Information Theory (2019).
- [2] Y. Li, C. Huang, L. Ding, Z. Li, Y. Pan, X. Gao, Deep learning in bioinformatics: Introduction, application, and perspective in the big data era, Methods 166 (2019) 4 – 21, deep Learning in Bioinformatics. doi:<https://doi.org/10.1016/j.ymeth.2019.04.008>.
- [3] R. Min, Machine Learning Approaches to Biological Sequence and Phenotype Data Analysis, University of Toronto, 2010.
- [4] M.-R. Cao, Z.-P. Han, J.-M. Liu, Y.-G. Li, Y.-B. Lv, J.-B. Zhou, J.-H. He, Bioinformatic analysis and prediction of the function and regulatory network of long non-coding rnas in hepatocellular carcinoma, Oncology letters 15 (5) (2018) 7783–7793.
- [5] W. J. d. S. Diniz, F. Canduri, Bioinformatics: an overview and its applications, Genet Mol Res 16 (1) (2017).

- [6] R. Parmezan Bonidia, A. C. Ponce de Leon Ferreira de Carvalho, A. Rossi Paschoal, D. Sipoli Sanches, Selecting the most relevant features for the identification of long non-coding rnas in plants, in: 2019 8th Brazilian Conference on Intelligent Systems (BRACIS), 2019, pp. 539–544. doi:10.1109/BRACIS.2019.00100.
- [7] V. I. Jurtz, A. R. Johansen, M. Nielsen, J. J. Almagro Armenteros, H. Nielsen, C. K. Sønderby, O. Winther, S. K. Sønderby, An introduction to deep learning on biological sequence data: examples and solutions, *Bioinformatics* 33 (22) (2017) 3685–3690. doi:10.1093/bioinformatics/btx531.
URL <https://doi.org/10.1093/bioinformatics/btx531>
- [8] S. Budach, A. Marsico, pysster: classification of biological sequences by learning sequence and structure motifs with convolutional neural networks, *Bioinformatics* 34 (17) (2018) 3035–3037. doi:10.1093/bioinformatics/bty222.
- [9] S. Min, B. Lee, S. Yoon, Deep learning in bioinformatics, *Briefings in Bioinformatics* 18 (5) (2016) 851–869. doi:10.1093/bib/bbw068.
- [10] Z. Chen, P. Zhao, F. Li, T. T. Marquez-Lago, A. Leier, J. Revote, Y. Zhu, D. R. Powell, T. Akutsu, G. I. Webb, K.-C. Chou, A. I. Smith, R. J. Daly, J. Li, J. Song, iLearn: an integrated platform and meta-learner for feature engineering, machine-learning analysis and modeling of DNA, RNA and protein sequence data, *Briefings in Bioinformatics* 21 (3) (2019) 1047–1057. doi:10.1093/bib/bbz041.
- [11] M. E. Maros, D. Capper, D. T. Jones, V. Hovestadt, A. von Deimling, S. M. Pfister, A. Benner, M. Zucknick, M. Sill, Machine learning workflows to estimate class probabilities for precision cancer diagnostics on dna methylation microarray data, *Nature Protocols* (2020) 1–34.
- [12] C. Ma, H. H. Zhang, X. Wang, Machine learning for big data analytics in plants, *Trends in Plant Science* 19 (12) (2014) 798 – 808. doi:<https://doi.org/10.1016/j.tplants.2014.08.004>.
- [13] J. Li, W. Liu, Puzzle of highly pathogenic human coronaviruses (2019-ncov), *Protein & Cell* (2020) 1–4.

- [14] D. Benvenuto, M. Giovanetti, A. Ciccozzi, S. Spoto, S. Angeletti, M. Ciccozzi, The 2019-new coronavirus epidemic: Evidence for virus evolution, *Journal of Medical Virology* 92 (4) (2020) 455–459. arXiv:<https://onlinelibrary.wiley.com/doi/pdf/10.1002/jmv.25688>, doi:10.1002/jmv.25688.
URL <https://onlinelibrary.wiley.com/doi/abs/10.1002/jmv.25688>
- [15] C. Xu, S. A. Jackson, BioSeq-Analysis: a platform for DNA, RNA and protein sequence analysis based on machine learning approaches, *Genome Biology* 20 (2019) 1–4. doi:<https://doi.org/10.1186/s13059-019-1689-0>.
URL <https://doi.org/10.1186/s13059-019-1689-0>
- [16] D. Storcheus, A. Rostamizadeh, S. Kumar, A survey of modern questions and challenges in feature extraction, in: *Feature Extraction: Modern Questions and Challenges*, 2015, pp. 1–18.
- [17] R. Saidi, S. Aridhi, E. M. Nguifo, M. Maddouri, Feature extraction in protein sequences classification: a new stability measure, in: *Proceedings of the ACM Conference on Bioinformatics, Computational Biology and Biomedicine*, ACM, 2012, pp. 683–689.
- [18] I. Guyon, S. Gunn, M. Nikravesh, L. A. Zadeh, *Feature extraction: foundations and applications*, Vol. 207, Springer, 2008.
- [19] J. Baek, B. Lee, S. Kwon, S. Yoon, Incrnanet: Long non-coding rna identification using deep learning, *Bioinformatics* 1 (2018) 9.
- [20] R. P. Bonidia, L. D. H. Sampaio, F. M. Lopes, D. S. Sanches, Feature extraction of long non-coding rnas: A fourier and numerical mapping approach, in: I. Nyström, Y. Hernández Heredia, V. Milián Núñez (Eds.), *Progress in Pattern Recognition, Image Analysis, Computer Vision, and Applications*, Springer International Publishing, Cham, 2019, pp. 469–479.
- [21] X. Pan, K. Xiong, Predcircrna: computational classification of circular rna from other long non-coding rna using hybrid features, *Molecular Biosystems* 11 (8) (2015) 2219–2226.
- [22] R. Muhammod, S. Ahmed, D. Md Farid, S. Shatabda, A. Sharma, A. Dehzangi, PyFeat: a Python-based effective feature generation tool

- for DNA, RNA and protein sequences, *Bioinformatics* 35 (19) (2019) 3831–3833. arXiv:<http://oup.prod.sis.lan/bioinformatics/article-pdf/35/19/3831/30061688/btz165.pdf>, doi:10.1093/bioinformatics/btz165. URL <https://doi.org/10.1093/bioinformatics/btz165>
- [23] Q. Abbas, S. M. Raza, A. A. Biyabani, M. A. Jaffar, A review of computational methods for finding non-coding rna genes, *Genes* 7 (12) (2016) 113.
 - [24] N. Amin, A. McGrath, Y.-P. P. Chen, Evaluation of deep learning in non-coding rna classification, *Nature Machine Intelligence* 1 (5) (2019) 246.
 - [25] Y.-J. Kang, D.-C. Yang, L. Kong, M. Hou, Y.-Q. Meng, L. Wei, G. Gao, Cpc2: a fast and accurate coding potential calculator based on sequence intrinsic features, *Nucleic acids research* 45 (W1) (2017) W12–W16.
 - [26] S. Han, Y. Liang, Q. Ma, Y. Xu, Y. Zhang, W. Du, C. Wang, Y. Li, Lncfinder: an integrated platform for long non-coding rna identification utilizing sequence intrinsic composition, structural information and physicochemical property, *Briefings in Bioinformatics* (2018).
 - [27] L. Chen, Y.-H. Zhang, G. Huang, X. Pan, S. Wang, T. Huang, Y.-D. Cai, Discriminating cirrnas from other lncrnas using a hierarchical extreme learning machine (h-elm) algorithm with feature selection, *Molecular Genetics and Genomics* 293 (1) (2018) 137–149.
 - [28] J. J. Quinn, H. Y. Chang, Unique features of long non-coding rna biogenesis and function, *Nature Reviews Genetics* 17 (1) (2016) 47.
 - [29] S. R. Eddy, Non-coding rna genes and the modern rna world, *Nature Reviews Genetics* 2 (12) (2001) 919.
 - [30] P. Kapranov, J. Cheng, S. Dike, D. A. Nix, R. Duttagupta, A. T. Willingham, P. F. Stadler, J. Hertel, J. Hackermüller, I. L. Hofacker, et al., Rna maps reveal new rna classes and a possible function for pervasive transcription, *Science* 316 (5830) (2007) 1484–1488.
 - [31] Y. Zhang, Y. Tao, Q. Liao, Long noncoding rna: a crosslink in biological regulatory network, *Briefings in bioinformatics* (2017).

- [32] A. Li, Q. Zang, D. Sun, M. Wang, A text feature-based approach for literature mining of lncrna–protein interactions, *Neurocomputing* 206 (2016) 73–80.
- [33] Y. Wang, Y. Li, Q. Wang, Y. Lv, S. Wang, X. Chen, X. Yu, W. Jiang, X. Li, Computational identification of human long intergenic non-coding rnas using a ga–svm algorithm, *Gene* 533 (1) (2014) 94–99.
- [34] L. Wang, L. Kuang, S. Ye, M. F. B. Iqbal, T. Pei, et al., A novel method for lncrna-disease association prediction based on an lncrna-disease association network, *IEEE/ACM Transactions on Computational Biology and Bioinformatics* (2018).
- [35] W. Zhang, Q. Qu, Y. Zhang, W. Wang, The linear neighborhood propagation method for predicting long non-coding rna–protein interactions, *Neurocomputing* 273 (2018) 526–534.
- [36] Q.-Z. Zhou, B. Zhang, Q.-Y. Yu, Z. Zhang, Bmncrnadb: a comprehensive database of non-coding rnas in the silkworm, *bombyx mori*, *BMC bioinformatics* 17 (1) (2016) 370.
- [37] M. Q. Hassan, C. E. Tye, G. S. Stein, J. B. Lian, Non-coding rnas: Epigenetic regulators of bone development and homeostasis, *Bone* 81 (2015) 746–756.
- [38] C. Ciaudo, N. Servant, V. Cognat, A. Sarazin, E. Kieffer, S. Viville, V. Colot, E. Barillot, E. Heard, O. Voinnet, Highly dynamic and sex-specific expression of micrornas during early es cell differentiation, *PLoS genetics* 5 (8) (2009) e1000620.
- [39] X. Peng, L. Gralinski, C. D. Armour, M. T. Ferris, M. J. Thomas, S. Proll, B. G. Bradel-Tretheway, M. J. Korth, J. C. Castle, M. C. Biery, et al., Unique signatures of long noncoding rna expression in response to virus infection and altered innate immune signaling, *MBio* 1 (5) (2010) e00206–10.
- [40] C. Pastori, C. Wahlestedt, Involvement of long noncoding rnas in diseases affecting the central nervous system, *RNA biology* 9 (6) (2012) 860–870.

- [41] Q. Zhang, Y. Wei, Z. Yan, C. Wu, Z. Chang, Y. Zhu, K. Li, Y. Xu, The characteristic landscape of lncrnas classified by rbp–lncrna interactions across 10 cancers, *Molecular bioSystems* 13 (6) (2017) 1142–1151.
- [42] H.-L. V. Wang, J. A. Chekanova, Long noncoding rnas in plants, in: *Long Non Coding RNA Biology*, Springer, 2017, pp. 133–154.
- [43] C. Di, J. Yuan, Y. Wu, J. Li, H. Lin, L. Hu, T. Zhang, Y. Qi, M. B. Gerstein, Y. Guo, et al., Characterization of stress-responsive lncrnas in arabidopsis thaliana by integrating expression, epigenetic and structural features, *The Plant Journal* 80 (5) (2014) 848–861.
- [44] D. Wang, Z. Qu, L. Yang, Q. Zhang, Z.-H. Liu, T. Do, D. L. Adelson, Z.-Y. Wang, I. Searle, J.-K. Zhu, Transposable elements (te s) contribute to stress-related long intergenic noncoding rna s in plants, *The Plant Journal* 90 (1) (2017) 133–146.
- [45] Y.-C. Zhang, J.-Y. Liao, Z.-Y. Li, Y. Yu, J.-P. Zhang, Q.-F. Li, L.-H. Qu, W.-S. Shu, Y.-Q. Chen, Genome-wide screening and functional analysis identify a large number of long noncoding rnas involved in the sexual reproduction of rice, *Genome biology* 15 (12) (2014) 512.
- [46] Y. Fang, M. J. Fullwood, Roles, functions, and mechanisms of long non-coding rnas in cancer, *Genomics, proteomics & bioinformatics* 14 (1) (2016) 42–54.
- [47] T. Derrien, R. Johnson, G. Bussotti, A. Tanzer, S. Djebali, H. Tilgner, G. Guernec, D. Martin, A. Merkel, D. G. Knowles, et al., The gene code v7 catalog of human long noncoding rnas: analysis of their gene structure, evolution, and expression, *Genome research* 22 (9) (2012) 1775–1789.
- [48] J. Cheng, P. Kapranov, J. Drenkow, S. Dike, S. Brubaker, S. Patel, J. Long, D. Stern, H. Tammana, G. Helt, et al., Transcriptional maps of 10 human chromosomes at 5-nucleotide resolution, *Science* 308 (5725) (2005) 1149–1154.
- [49] L. Ma, V. B. Bajic, Z. Zhang, On the classification of long non-coding rnas, *RNA biology* 10 (6) (2013) 924–933.

- [50] R. Hu, X. Sun, Lncrnatargets: a platform for lncrna target prediction based on nucleic acid thermodynamics, *Journal of bioinformatics and computational biology* 14 (04) (2016) 1650016.
- [51] S. Chooniedass-Kothari, E. Emberley, M. Hamedani, S. Troup, X. Wang, A. Czosnek, F. Hube, M. Mutawe, P. Watson, E. Leygue, The steroid receptor rna activator is the first functional rna encoding a protein, *FEBS letters* 566 (1-3) (2004) 43–47.
- [52] Y. He, X.-M. Meng, C. Huang, B.-M. Wu, L. Zhang, X.-W. Lv, J. Li, Long noncoding rnas: Novel insights into hepatocellular carcinoma, *Cancer letters* 344 (1) (2014) 20–27.
- [53] J. T. Kung, D. Colognori, J. T. Lee, Long noncoding rnas: past, present, and future, *Genetics* 193 (3) (2013) 651–669.
- [54] L. Kong, Y. Zhang, Z.-Q. Ye, X.-Q. Liu, S.-Q. Zhao, L. Wei, G. Gao, Cpc: assess the protein-coding potential of transcripts using sequence features and support vector machine, *Nucleic acids research* 35 (suppl_2) (2007) W345–W349.
- [55] L. Wang, H. J. Park, S. Dasari, S. Wang, J.-P. Kocher, W. Li, Cpat: Coding-potential assessment tool using an alignment-free logistic regression model, *Nucleic acids research* 41 (6) (2013) e74–e74.
- [56] L. Sun, H. Luo, D. Bu, G. Zhao, K. Yu, C. Zhang, Y. Liu, R. Chen, Y. Zhao, Utilizing sequence intrinsic composition to classify protein-coding and long non-coding transcripts, *Nucleic acids research* 41 (17) (2013) e166–e166.
- [57] A. Li, J. Zhang, Z. Zhou, Plek: a tool for predicting long non-coding rnas and messenger rnas based on an improved k-mer scheme, *BMC bioinformatics* 15 (1) (2014) 311.
- [58] X.-N. Fan, S.-W. Zhang, Lncrna-mfdl: identification of human long non-coding rnas by fusing multiple features and using deep learning, *Molecular BioSystems* 11 (3) (2015) 892–897.
- [59] R. Achawanantakun, J. Chen, Y. Sun, Y. Zhang, Lncrna-id: Long non-coding rna identification using balanced random forests, *Bioinformatics* 31 (24) (2015) 3897–3905.

- [60] L. Sun, H. Liu, L. Zhang, J. Meng, Lncrscan-svm: a tool for predicting long non-coding rnas using support vector machine, *PloS one* 10 (10) (2015) e0139654.
- [61] C. Pian, G. Zhang, Z. Chen, Y. Chen, J. Zhang, T. Yang, L. Zhang, Lncrnapped: Classification of long non-coding rnas and protein-coding transcripts by the ensemble algorithm with a new hybrid feature, *PloS one* 11 (5) (2016) e0154567.
- [62] R. Tripathi, S. Patel, V. Kumari, P. Chakraborty, P. K. Varadwaj, Deeplnc, a long non-coding rna prediction tool using deep neural network, *Network Modeling Analysis in Health Informatics and Bioinformatics* 5 (1) (2016) 21.
- [63] L. M. Vieira, C. Grativil, F. Thiebaut, T. G. Carvalho, P. R. Hardoim, A. Hemerly, S. Lifschitz, P. C. G. Ferreira, M. E. M. Walther, Plantrna_sniffer: a svm-based workflow to predict long intergenic non-coding rnas in plants, *Non-coding RNA* 3 (1) (2017) 11.
- [64] U. Singh, N. Khemka, M. S. Rajkumar, R. Garg, M. Jain, Plncpro for prediction of long non-coding rnas (lncrnas) in plants and its application for discovery of abiotic stress-responsive lncrnas in rice and chickpea, *Nucleic acids research* 45 (22) (2017) e183–e183.
- [65] T. d. C. Negri, W. A. L. Alves, P. H. Bugatti, P. T. M. Saito, D. S. Domingues, A. R. Paschoal, Pattern recognition analysis on long non-coding rnas: a tool for prediction in plants, *Briefings in bioinformatics* (2018).
- [66] E. A. Ito, I. Katahira, F. F. d. R. Vicente, L. F. P. Pereira, F. M. Lopes, Basinet—biological sequences network: a case study on coding and non-coding rnas identification, *Nucleic acids research* (2018).
- [67] C. M. Simopoulos, E. A. Weretilnyk, G. B. Golding, Prediction of plant lncrna by ensemble machine learning classifiers, *BMC genomics* 19 (1) (2018) 316.
- [68] J.-C. Guo, S.-S. Fang, Y. Wu, J.-H. Zhang, Y. Chen, J. Liu, B. Wu, J.-R. Wu, E.-M. Li, L.-Y. Xu, L. Sun, Y. Zhao, CNIT: a fast and accurate web tool for identifying protein-coding and long non-coding

- transcripts based on intrinsic sequence composition, Nucleic Acids Research 47 (W1) (2019) W516–W522. doi:10.1093/nar/gkz400.
- [69] S. Deshpande, J. Shuttleworth, J. Yang, S. Taramonli, M. England, Plit: An alignment-free computational tool for identification of long non-coding rnas in plant transcriptomic datasets, Computers in Biology and Medicine 105 (2019) 169 – 181. doi:<https://doi.org/10.1016/j.combiomed.2018.12.014>.
 - [70] S. Liu, X. Zhao, G. Zhang, W. Li, F. Liu, S. Liu, W. Zhang, Predlnc-gfstack: A global sequence feature based on a stacked ensemble learning method for predicting lncrnas from transcripts, Genes 10 (9) (2019) 672.
 - [71] G. Wang, H. Yin, B. Li, C. Yu, F. Wang, X. Xu, J. Cao, Y. Bao, L. Wang, A. A. Abbasi, V. B. Bajic, L. Ma, Z. Zhang, Characterization and identification of long non-coding RNAs based on feature relationship, Bioinformatics 35 (17) (2019) 2949–2956. doi:10.1093/bioinformatics/btz008.
 - [72] Y. Zhang, C. Jia, M. J. Fullwood, C. K. Kwoh, DeepCPP: a deep neural network based on nucleotide bias information and minimum distribution similarity feature selection for RNA coding potential prediction, Briefings in Bioinformatics (03 2020). doi:10.1093/bib/bbaa039.
 - [73] S. F. Altschul, T. L. Madden, A. A. Schäffer, J. Zhang, Z. Zhang, W. Miller, D. J. Lipman, Gapped blast and psi-blast: a new generation of protein database search programs, Nucleic acids research 25 (17) (1997) 3389–3402.
 - [74] A. C. Liu, The effect of oversampling and undersampling on classifying imbalanced text datasets, The University of Texas at Austin (2004).
 - [75] D. M. Goodstein, S. Shu, R. Howson, R. Neupane, R. D. Hayes, J. Fazo, T. Mitros, W. Dirks, U. Hellsten, N. Putnam, et al., Phytozome: a comparative platform for green plant genomics, Nucleic acids research 40 (D1) (2011) D1178–D1186.
 - [76] A. Paytuví Gallart, A. Hermoso Pulido, I. Anzar Martínez de Lagrán, W. Sanseverino, R. Aiese Cigliano, Greenc: a wiki-based database of plant lncrnas, Nucleic acids research 44 (D1) (2015) D1161–D1166.

- [77] D. Chen, C. Yuan, J. Zhang, Z. Zhang, L. Bai, Y. Meng, L.-L. Chen, M. Chen, PlantNATsDB: a comprehensive database of plant natural antisense transcripts, *Nucleic Acids Research* 40 (D1) (2011) D1187–D1193. arXiv:<https://academic.oup.com/nar/article-pdf/40/D1/D1187/9481672/gkr823.pdf>, doi:10.1093/nar/gkr823. URL <https://doi.org/10.1093/nar/gkr823>
- [78] Q. Chu, X. Zhang, X. Zhu, C. Liu, L. Mao, C. Ye, Q.-H. Zhu, L. Fan, Plantcircbase: a database for plant circular rnas, *Molecular plant* 10 (8) (2017) 1126–1128.
- [79] C. Yin, Y. Chen, S. S.-T. Yau, A measure of dna sequence similarity by fourier transform with applications on hierarchical clustering, *Journal of theoretical biology* 359 (2014) 18–28.
- [80] C. Yin, S. S.-T. Yau, A fourier characteristic of coding sequences: origins and a non-fourier approximation, *Journal of computational biology* 12 (9) (2005) 1153–1165.
- [81] D. Anastassiou, Genomic signal processing, *IEEE signal processing magazine* 18 (4) (2001) 8–20.
- [82] L. Marsella, F. Sirocco, A. Trovato, F. Seno, S. C. Tosatto, Repetita: detection and discrimination of the periodicity of protein solenoid repeats by discrete fourier transform, *Bioinformatics* 25 (12) (2009) i289–i295.
- [83] W. T. Cochran, J. W. Cooley, D. L. Favin, H. D. Helms, R. A. Kaenel, W. W. Lang, G. C. Maling, D. E. Nelson, C. M. Rader, P. D. Welch, What is the fast fourier transform?, *Proceedings of the IEEE* 55 (10) (1967) 1664–1674.
- [84] M. Abo-Zahhad, S. M. Ahmed, S. A. Abd-Elrahman, Genomic analysis and classification of exon and intron sequences using dna numerical mapping techniques, *International Journal of Information Technology and Computer Science* 4 (8) (2012) 22–36.
- [85] G. Mendizabal-Ruiz, I. Román-Godínez, S. Torres-Ramos, R. A. Salido-Ruiz, J. A. Morales, On dna numerical representations for genomic similarity computation, *PloS one* 12 (3) (2017) e0173288.

- [86] R. F. Voss, Evolution of long-range fractal correlations and 1/f noise in dna base sequences, *Physical review letters* 68 (25) (1992) 3805.
- [87] P. D. Cristea, Conversion of nucleotides sequences into genomic signals, *Journal of cellular and molecular medicine* 6 (2) (2002) 279–303.
- [88] N. Chakravarthy, A. Spanias, L. D. Iasemidis, K. Tsakalis, Autoregressive modeling and feature analysis of dna sequences, *EURASIP Journal on Applied Signal Processing* 2004 (2004) 13–28.
- [89] R. Zhang, C.-T. Zhang, Z curves, an intutive tool for visualizing and analyzing the dna sequences, *Journal of Biomolecular Structure and Dynamics* 11 (4) (1994) 767–782.
- [90] A. S. Nair, S. P. Sreenadhan, A coding measure scheme employing electron-ion interaction pseudopotential (eiip), *Bioinformation* 1 (6) (2006) 197.
- [91] D. Anastassiou, Genomic signal processing, *IEEE Signal Processing Magazine* 18 (4) (2001) 8–20. doi:10.1109/79.939833.
- [92] N. Yu, Z. Li, Z. Yu, Survey on encoding schemes for genomic data representation and feature learning—from signal processing to machine learning, *Big Data Mining and Analytics* 1 (3) (2018) 191–210.
- [93] J. Shao, X. Yan, S. Shao, Snr of dna sequences mapped by general affine transformations of the indicator sequences, *Journal of mathematical biology* 67 (2) (2013) 433–451.
- [94] C.-T. Zhang, A symmetrical theory of dna sequences and its applications, *Journal of theoretical biology* 187 (3) (1997) 297–306.
- [95] C. Yin, S. S.-T. Yau, Prediction of protein coding regions by the 3-base periodicity analysis of a dna sequence, *Journal of theoretical biology* 247 (4) (2007) 687–694.
- [96] H. Nikookar, Peak-to-average power ratio, in: *Wavelet Radio: Adaptive and Reconfigurable Wireless Systems Based on Wavelets*, Cambridge University Press, 2013, pp. 93–111. doi:10.1017/CBO9781139084697.006.

- [97] I. Pritišanac, R. M. Vernon, A. M. Moses, J. D. Forman Kay, Entropy and information within intrinsically disordered protein regions, *Entropy* 21 (7) (2019) 662.
- [98] S. Vinga, Information theory applications for biological sequence analysis, *Briefings in bioinformatics* 15 (3) (2013) 376–389.
- [99] J. T. Machado, A. C. Costa, M. D. Quelhas, Shannon, rényie and tsallis entropy analysis of dna using phase plane, *Nonlinear Analysis: Real World Applications* 12 (6) (2011) 3135–3144.
- [100] A. Lesne, Shannon entropy: a rigorous notion at the crossroads between probability, information theory, dynamical systems and statistical physics, *Mathematical Structures in Computer Science* 24 (3) (2014).
- [101] M. P. De Albuquerque, I. A. Esquef, A. G. Mello, Image thresholding using tsallis entropy, *Pattern Recognition Letters* 25 (9) (2004) 1059–1065.
- [102] F. M. Lopes, E. A. de Oliveira, R. M. Cesar, Inference of gene regulatory networks from time series by tsallis entropy, *BMC systems biology* 5 (1) (2011) 61.
- [103] A. Ramírez-Reyes, A. R. Hernández-Montoya, G. Herrera-Corral, I. Domínguez-Jiménez, Determining the entropic index q of tsallis entropy in images through redundancy, *Entropy* 18 (8) (2016) 299.
- [104] L. d. F. Costa, F. A. Rodrigues, A. S. Cristino, Complex networks: the key to systems biology, *Genetics and Molecular Biology* 31 (3) (2008) 591–601.
- [105] X. F. Wang, Complex networks: topology, dynamics and synchronization, *International journal of bifurcation and chaos* 12 (05) (2002) 885–916.
- [106] B. K. Singh, K. Verma, A. Thoke, Investigations on impact of feature normalization techniques on classifier’s performance in breast tumor classification, *International Journal of Computer Applications* 116 (19) (2015).

- [107] M. C. de Souto, D. S. de Araujo, I. G. Costa, R. G. Soares, T. B. Ludermir, A. Schliep, Comparative study on normalization procedures for cluster analysis of gene expression datasets, in: Neural Networks, 2008. IJCNN 2008.(IEEE World Congress on Computational Intelligence). IEEE International Joint Conference on, IEEE, 2008, pp. 2792–2798.
- [108] L. Breiman, Random forests, *Machine learning* 45 (1) (2001) 5–32.
- [109] T. Hastie, S. Rosset, J. Zhu, H. Zou, Multi-class adaboost, *Statistics and its Interface* 2 (3) (2009) 349–360.
- [110] A. V. Dorogush, V. Ershov, A. Gulin, Catboost: gradient boosting with categorical features support, arXiv preprint arXiv:1810.11363 (2018).
- [111] J. Cohen, A coefficient of agreement for nominal scales, *Educational and psychological measurement* 20 (1) (1960) 37–46.